1) UNCLASSIFIED

2

AD-A206 021

DOCUMENTATION PAGE

Form Approved
OMB No. 0704-0188

1b. RESTRICTIVE MARKINGS

3. DISTRIBUTION/AVAILABILITY OF REPORT
Approved for Public Release
Distribution Unlimited

2b. DECLASSIFICATION/DOWNGRADING SCHEDULE

4. PERFORMING ORGANIZATION REPORT NUMBER(S)

5. MONITORING ORGANIZATION REPORT NUMBER(S)
AFOSR-TR- 89-0304

6a. NAME OF PERFORMING ORGANIZATION	6b. OFFICE SYMBOL (If applicable)	7a. NAME OF MONITORING ORGANIZATION
Stanford University		AFOSR/NA

6c. ADDRESS (City, State, and ZIP Code)	7b. ADDRESS (City, State, and ZIP Code)
Mechanical Engineering Dept. Stanford, CA 94305	Building 410 Bolling Air Force Base, D.C. 20332-6448

8a. NAME OF FUNDING/SPONSORING ORGANIZATION	8b. OFFICE SYMBOL (If applicable)	9. PROCUREMENT INSTRUMENT IDENTIFICATION NUMBER
AFOSR	NA	AFOSR-88-0056

8c. ADDRESS (City, State, and ZIP Code)	10. SOURCE OF FUNDING NUMBERS			
	PROGRAM ELEMENT NO.	PROJECT NO.	TASK NO	WORK UNIT ACCESSION NO.
Building 410 Bolling Air Force Base, D.C. 20332-6448	61102F	2307	A2	

11. TITLE (Include Security Classification)
Strange Attractor Dimensions in Poiseuille Flow

12. PERSONAL AUTHOR(S)
Moin, Parviz

13a. TYPE OF REPORT	13b. TIME COVERED	14. DATE OF REPORT (Year, Month, Day)	15. PAGE COUNT
Final	FROM 12/1/87 TO 1/30/89	89/2/13	30

16. SUPPLEMENTARY NOTATION

17. COSATI CODES			18. SUBJECT TERMS (Continue on reverse if necessary and identify by block number)
FIELD	GROUP	SUB-GROUP	Turbulence, Strange Attractor, Channel Flow

19. ABSTRACT (Continue on reverse if necessary and identify by block number)

It is shown that fully developed channel flow is confined to a strange attractor. However, the dimension of the attractor is much larger than dimensions encountered in closed flows such as Benard Convection and Taylor-Couette flow. In addition, we have examined the relationship between turbulent structures and attractor geometry.

20. DISTRIBUTION/AVAILABILITY OF ABSTRACT	21. ABSTRACT SECURITY CLASSIFICATION
☒ UNCLASSIFIED/UNLIMITED ☐ SAME AS RPT ☐ DTIC USERS	Unclassified

22a. NAME OF RESPONSIBLE INDIVIDUAL	22b. TELEPHONE (Include Area Code)	22c. OFFICE SYMBOL
James M. McMichael	(202) 767-4936	NA

DD Form 1473, JUN 86 — Previous editions are obsolete. — SECURITY CLASSIFICATION OF THIS PAGE

UNCLASSIFIED

Final Report: AFOSR-88-0056

THE DIMENSION OF ATTRACTORS UNDERLYING TURBULENT POISEUILLE FLOW

Laurence Keefe and Parviz Moin

Mechanical Engineering Dept., Stanford University, Stanford, CA 94305

INTODUCTION

Is the "strange attractor" the correct mathematical model for fully developed turbulent flows? We believe that our research, described below, has successfully provided an affirmative answer to this question. Nonlinear dynamical systems theory excites interest as a turbulence theory because it provides an explicit mathematical framework to connect the chaotic, time dependent dynamics of real flows to the structure of the Navier-Stokes(NS) equations. The theory demonstrates that:

- The dynamics of dissipative systems (of which turbulence is one) are often confined to strange attractors.
- Such attractors carry within their intrinsic structure a well defined mechanism(usually called "sensitive dependence on initial conditions") that can produce chaotic and unpredictable behavior in all physical systems, without requiring random forcing.
- If fully developed turbulence is confined to a strange attractor, it is describable by a finite number of degrees of freedom, despite the NS equations being infinite dimensional. This has encouraged hope that the turbulence problem can be reduced in apparent complexity by projecting it onto some special basis.
- It is not a statistical theory. Statistical theories take the nonlinear NS equations and tranform them into stochastic, linear equations. Any random behavior in these equations can be traced explicitly to the stochastic model used to replace the nonlinear terms in the NS equations.
- Chaos theory does not <u>model</u> turbulent dynamics, it <u>analyzes</u> them. The dynamics of the system are governed by the full NS equations and randomness results from the explicit nonlinearities in the equation, not some random model of them. By doing so it has given the first real clue as to the origins of randomness in fluid turbulence.

In the end, what is sought from any theory of turbulence is a universal framework that allows known phenomena to be understood, calculated, and related, and a predictive capability for unknown flows or control measures. Crucial to the erection of such a structure is a knowledge of the fundamental mathematical character of turbulence. The purpose of this research has been to investigate this character to determine if chaos theory and the strange attractor can provide the foundation

for such a global theory.

PREVIOUS WORK

There is much theoretical and experimental work[1-6] that establishes chaos theory as the underlying mathematics of closed flows such as Bénard convection and Taylor-Couette flow. Our work is one of the first to establish links between chaos theory and a complex, fully developed, turbulent flow of aerodynamic interest. Our preliminary results on dimension, reported with our original proposal, were obtained from low resolution simulations of channel flow that reproduced calculations reported in the literature[7]. We now believe the cited work to be incorrect. At worst, the "turbulence" computed there is completely spurious, totally an artefact of the numerics. At best, its characteristics so strongly depend on simulation parameters, such as timestep, that no one is likely to consider the results reliable. As a result of this painful discovery we have had to redo the dimension calculation at a higher Reynolds number and resolution, after exhaustively establishing a new simulation of the channel flow which does not suffer from the same defects as the one we originally reproduced. It is these new results that we report here.

RESULTS

Our research program has developed along two lines. The first has been the dimension calculation originally proposed. As an outgrowth of our work there we opened a second, and began studying the relation between the structure of attractors and the turbulent phenomena they represent. This latter will be discussed briefly below.

Our primary research has established the first strong evidence that the turbulent solutions of the NS equations are confined to a strange attractor. At a single Reynolds number in turbulent channel flow we have determined the dimension, D_λ, of the underlying attractor, having measured sufficient of the Lyapunov exponent hierarchy, λ_i, to calculate this quantity from the Kaplan-Yorke[8] definition:

$$D_\lambda = j + |\lambda_{j+1}|^{-1} \sum_{i=1}^{j} \lambda_i \ ,$$

where $\sum_{i=1}^{j} \lambda_i > 0, \qquad \sum_{i=1}^{j+1} \lambda_i < 0.$

The results of the calculation are displayed in Figure 1, where the values of the Lyapunov exponents λ_i are plotted against their index i. The first 450 exponents

were calculated, at a cost of some 400 hours of cpu time on a CRAY 2. During this time the basic flow convected almost 1300 channel half widths. The slight non-uniformities in the distribution result from some lack of convergence of the exponent values even after these long time scales. Application of the Kaplan-Yorke formula to this distribution yields a dimension of $D_\lambda \simeq 360$, and a metric entropy $h_\mu \simeq 97$. The first 166 exponents are positive. Though the computational grid is $16 \times 33 \times 8$, and there are three velocity components at each node, particular features of the flow solver reduce the independent nodes to $15 \times 33 \times 7$, and the incompresibility of the flow means that only two of the velocity components are independent. Thus there are $15 \times 33 \times 7 \times 2 = 6930$ degrees of freedom in the calculation, and the attractor dimension is roughly 6% of the dimension of the complete phase space.

Calculating the dimension of the solution attractor measures the number of degrees of freedom needed to characterize a point on the attractor, and is a direct measure of the intrinsic complexity of the turbulence. Of the several definitions[9,10] of dimension available, we have chosen to use the Kaplan-Yorke formula(which bounds the fractal dimension[11]), since we have access to the dynamical equations(the NS equations) of the system, and can calculate the Lyapunov exponent hierarchy. This is in contrast to the one previous attempt[12] to calculate the dimension of attractors in Poiseuille flow, which employed methods most suited to data derived from experiments. This attempt failed, concluding that the dimension is greater than 40. Because our calculations indicate the dimension is almost an order of magnitude greater than 40, it is clear that none of the "experimental" methods for measuring dimension can be expected to work on this problem, because the data required exceeds current computer storage capabilities. This is true whether the method is a variant of the "correlation" dimension,[10] or is one of the newer techniques[13,14] to calculate the Lyapunov exponents experimentally.

The Lyapunov exponents of turbulent Poiseuille flow were calculated using standard[15] methods. The core of the algorithm was a flow solver written to perform full numerical simulation of low Reynolds number, channel flow.[16] The periodic application of a Gram-Schmidt orthogonalization to the separation vectors, required by the algorithm, has been checked to verify that the cosine of the angle between any two orthogonalized members of the set was never greater in magnitude than 10^{-11}. Numerical applications of the Gram-Schmidt process are known to be susceptible

to round-off errors when one begins with N vectors in an N-dimensional space and seeks to obtain N mutually orthogonal vectors from them. **Such is not the case here, for the dimension of the phase space is 6930 and, at most, we seek 450 mutually orthogonal directions in that space.**

The flow conditions for which the dimension was calculated correspond to a Reynolds number R_p, based on pressure gradient($=|\nabla p|L^3/2\rho\nu^2$, p= pressure, L=channel half-width, ρ=density, ν=kinematic viscosity) of 3200. This corresponds to a Reynolds number Re_τ, based on wall scaling, of 80. It is below the value where the laminar flow becomes linearly unstable($R_p = 5772$), and in the region($R_p \simeq 2900$) where it becomes unstable to finite-amplitude, two-dimensional disturbances. The simulated flow is definitely chaotic, and does a good job of predicting the mean velocity profile and turbulent intensities, but is a poorly resolved simulation in the sense that the computational grid in planes parallel to the channel walls is sparse(16×8), even though it is better resolved (33 points) in the direction perpendicular to the walls. This Reynolds number is near the minimum for which turbulent channel flow can be sustained . The restricted range of spatial scales resolved, as well as the small domain of the calculation, lead us to believe that our results are a lower bound on the true dimension of the flow at this Reynolds number. However, the proof of this contention awaits completion of calculations at both increased resolutions and domain size. Unlike results found in two-dimensional Bénard simulations[17], **we know that there is no "return to order" as resolution is increased at this Reynolds number.**

The second line of research has been devoted to relating turbulent structure to attractor geometry. Expanding on previous suggestions[18], a geometrical interpretation of conditional sampling schemes in the phase space of the attractor has shown how "coherent structures" naturally result from the exponential divergence property of the attractor underlying fully developed turbulence. This point has been demonstrated first with the Lorenz system and then using both the VITA and Quadrant techniques on velocity fields computed from channel simulations. Any conditional sampling scheme establishes a "window" in phase space that selects a bundle of trajectories on the turbulent attractor for averaging. The exponential divergence property then guarantees that this averaging process yields a finite size structure. At the same time it is clear that many such "windows" are possible, and

each has a "structure" associated with it. This geometrical interpretation in phase space explains not only why conditional sampling schemes work, but also why they have problems. These ideas are elaborated in the Appendix, which is a copy of a paper presented at the International Seminar on Near-Wall Turbulence, Dubrovnik, Yugoslavia, May 1988.

IMPLICATIONS

The results described above are important for many current studies of fluid turbulence. Foremost, we believe that **we have supplied the first strong evidence that fully developed turbulent solutions to the Navier-Stokes equations are confined to a finite-dimensional, strange, attractor.** This implies several things:

- Time randomness in fluids results from the "sensitive dependence ..." mechanism intrinsic to such attractors.
- The intrinsic complexity of turbulence has finally been measured. Though the dimension of the attractor is finite, its magnitude places this dynamical system in an entirely different class from those analyzed experimentally in the Bénard or Taylor-Couette problems. **Shear turbulence cannot be considered to result from the interactions of a few degrees of freedom.**
- For experimentalists the news is largely negative. No available method of calculating dimension from measured data can handle a dimension so high. The number of points required for the "correlation" dimension,[10] if the scaling region is to extend over only a factor of 2, is 10^{108} ! A billion points would give a scaling region within a radius variation of only 6%. Thus there was no chance that the previous attempt[12] to calculate dimension by these methods could have succeeded.
- Methods suitable for analysis of low-dimensional systems will encounter severe difficulties in the turbulence problem. Even assuming that a 360-dimensional system of equations can be found, say by using Karhunen-Loeve decomposition methods[19,20], the resultant dynamical system is still likely to be too complex for analysis. Simply extracting the fixed points of a 360^{th} order system is a non-trivial task. And the subsequent analysis of phase space orbits in terms of these singularities is daunting even to contemplate. Thus it seems unlikely,

given the dimension of the attractor, that even a 40 mode truncation could get the basic, qualitative dynamics of the full system correct, though this remains to be demonstrated. New analysis methods must be developed for such high dimensional systems.

FUTURE WORK

One of the promises of dynamical systems theory has been to predict the physics of systems from the geometry of their solutions in phase space. This is no more than a statement that the physical phenomena in a system must find expression or origin in the mathematical structure of its underlying solution attractor. With the strange attractor established as the underlying mathematical structure of shear turbulence, there is now a wealth of possibilities for perceptive linking of its geometry to actual flow phenomena. Our efforts using these methods have already met with some success(see previously mentioned appendix), by establishing a connection between the exponential divergence properties of such attractors and experimentally observed "coherent structures"[21]. This is just the first step in a process which promises to provide insight into the global properties of turbulence by studying the geometry of its attractor. Some other possibilities are outlined below.

Both the Renormalization Group Theory(RNG)[22] approach to turbulence as well as the large eddy simulation technique implicitly assume that, beyond some wavenumber, the effect of turbulent eddies is just to cascade energy from larger scales and dampen it, without affecting the fundamental dynamics of the larger scales. A study of dimension versus resolution will provide new information on the scale at which this common assumption becomes justified. Until the dimension stops changing with resolution there is doubt that the fundamental dynamical mechanisms in the flow are being modeled correctly, since addition of scales complicates[23] or simplifies[17] them further. If, however, the dimension asymptotes quickly with scale, this may help justify the use of coarser simulations and modeling to study the qualitative dynamics of a flow even when its quantitative aspects(skin friction, Reynolds stress distribution etc.) are in error. In essence we will study the structural stability of Navier-Stokes solutions to the addition of small scales.

Definitions of "coherent structure" are almost as numerous as the people who have measured them. Our work[21] has led to a deeper understanding of this arbtrariness, and shown that "structure" can be found at any time in a turbulent flow.

Since geometry led us to the realization that there is structure everywhere on the attractor, it is natural to ask if geometry can lead us to a finer, more restrictive, definition of "coherent structure". The question being asked here is: Are any points on the attractor special? And do the flow structures defined by the neighborhood of these points have a transparent physical interpretation?

Finally, the geometry of attractors may give new insights into the turbulence modeling problem. Reynolds-averaging the NS equations is equivalent to the geometric operation in phase space of finding the centroid of a flow's strange attractor. Is there another set of operations in phase space which will find this centroid without Reynolds-averaging? A study of the geometry of solutions to the Reynolds-averaged equations and their relation to the attractors of the unaveraged equations might reveal such a link .

PRESENTATIONS AND PUBLICATIONS

Both our work on the calculation of dimension and on the relation of coherent structures to strange attractors is in preparation for submission to journals. The dimension calculation has already been described in several public forums. Along with seminars at both Stanford and Brown, the dimension work was presented at the APS Fluid Dynamics meeting at Eugene, OR. in 1987, and most recently as an invited talk at the annual meeting of the American Association for the Advancement of Science (AAAS) in San Francisco, January 1989. A manuscript of that talk is to appear in a forthcoming book published by AAAS. The coherent structures work was originally presented at the 1987 APS meeting, and, in much expanded form, at the International Seminar on Near-Wall Turbulence, Dubrovnik, Yugoslavia, May 1988. It will also appear in the proceedings of that conference.

REFERENCES

1. J.P. Gollub and S.V. Benson, J.Fluid Mech. **100**, 449(1980).
2. A. Libchaber, S. Fauve, and C. Laroche, Physica **7D**, 73(1983).
3. M. Gorman, P.J. Widmann, and K.A. Robbins, Physica **19D**, 253(1986).
4. D.R. Moore, J. Toomre, E. Knobloch, and N.O. Weiss, Nature **303**, 663(1983).
5. F.H. Busse, in *Hydrodynamic Instabilities and the Transition to Turbulence* (Springer-Verlag, 1981), p292.
6. A. Brandstater and H.L. Swinney, Phys. Rev. A **35**, 2207(1987).
7. B.L. Rozhdestvensky, and I.N. Simakin, J. Fluid Mech. **147**, 261(1984).
8. J.L. Kaplan, J.A. Yorke, in *Functional Differential Equations and Approximations of Fixed Points*(Springer-Verlag, 1979), p228.
9. J.D. Farmer, E. Ott, and J.A. Yorke, Physica **7D**, 153(1983).
10. P. Grassberger and I. Procaccia, Physica **9D**, 189(1983).
11. P. Constantin and C. Foias, Comm. Pure Appl. Math. **38**, 1(1985).
12. A. Brandstadter, H.L. Swinney, and G.T. Chapman, in *Entropies and Dimensions in Chaotic Systems*(Springer-Verlag, 1986).
13. J.-P. Eckmann and D. Ruelle, Rev. Mod. Phys. **57**, 617(1985).
14. D.S. Broomhead and G.P. King, in *Nonlinear Phenomena and Chaos*(Adam Hilger, 1986).
15. G. Benettin, L. Galgani, A. Giorgilli, and J.-M. Strelcyn, Meccanica, **15**, 9(1980).
16. J. Kim, P. Moin, and R. Moser, J. Fluid Mech. **177**, 133(1987).
17. J.H. Curry, J.R. Herring, J. Loncaric, and S.A. Orszag, J. Fluid Mech. **147**, 1(1984).
18. L.R. Keefe, Ph.D. Thesis, University of Southern California, 1984.
19. J.L. Lumley, in *Transition and Turbulence*(Academic Press, 1981).
20. N. Aubry, P. Holmes, J.L. Lumley, and E.Stone, J. Fluid Mech. **192** , 115(1988)
21. L.R. Keefe, To be published in the proceedings of the International Seminar on Near-Wall Turbulence, Dubrovnik, Yugoslavia, May 1988
22. V. Yakhot, S.A. Orszag, J. Sci. Comp. **1**, 1986, p3
23. V. Franceschini, C. Tebaldi J. Stat. Phys. **25**, 1981, p397

Figure Captions

Figure 1. Distribution of Lyapunov exponents, λ_i

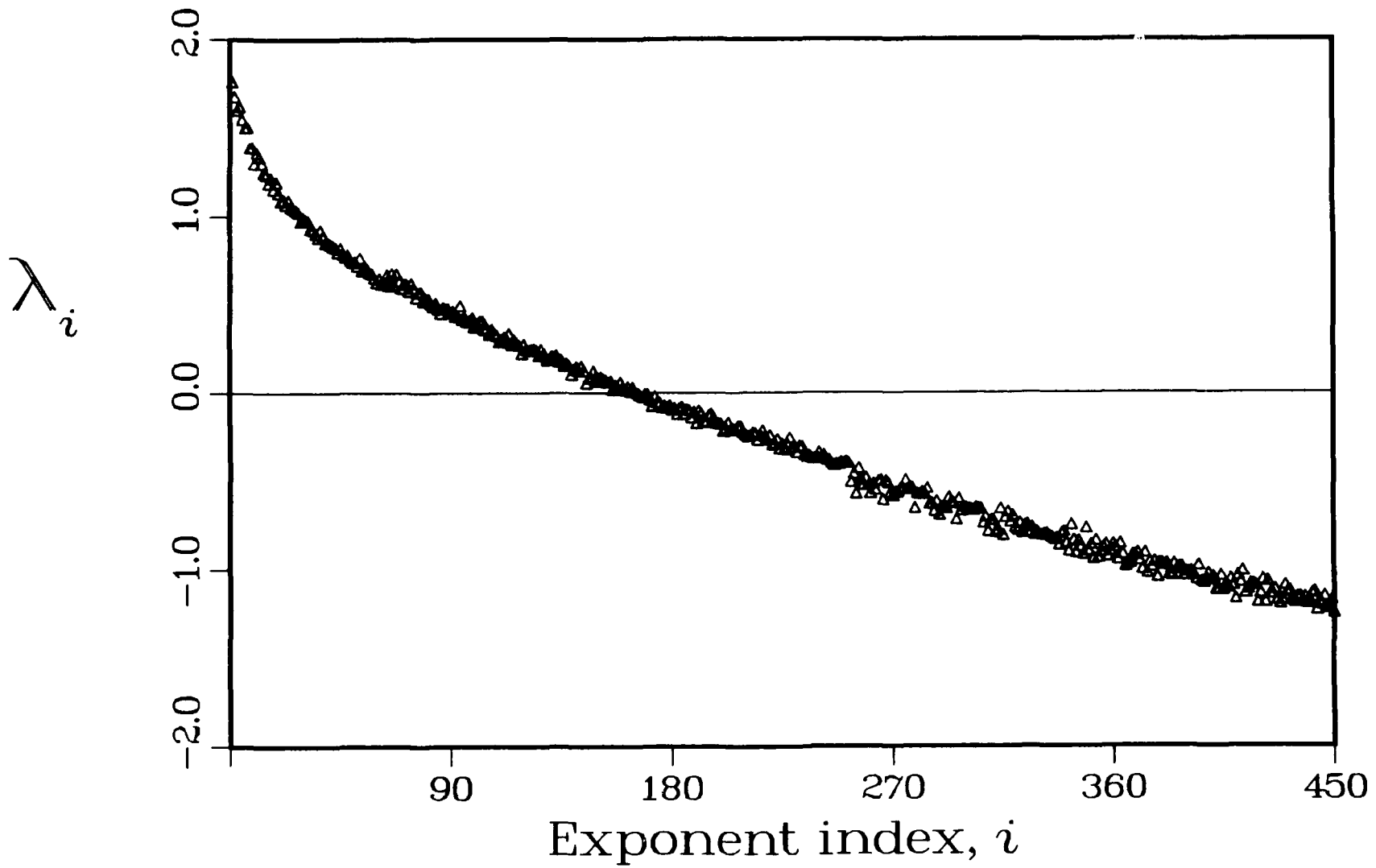
λ_i
2.0
1.0
0.0
−1.0
−2.0
90
180
270
360
450
Exponent index, i

APPENDIX

CONNECTING COHERENT STRUCTURES AND STRANGE ATTRACTORS

By Laurence R. Keefe

Center for Turbulence Research, NASA Ames Research Center, Moffett Field, CA 94035, and Stanford University, Stanford, CA 94305

INTRODUCTION

The current belief in "coherent structures" is a synthesis of two historically persistent notions of turbulence. On the one hand has been the perception that turbulence is a stochastic process, while on the other has been the recognition that "eddies", identifiable structures within the stochastic stew, are ubiquitous in shear turbulence under all conditions. From these two views emerges the belief that turbulence contains structures, similar in character, but random in occurrence, whose dynamics strongly influence evolution of the flow.

A third view of turbulence, neither historic, nor yet persistent,(nor even widely accepted!) derives from nonlinear dynamical systems theory. This theory suggests that turbulent solutions to the Navier-Stokes equations are confined to "strange attractors", and, by implication, that turbulent phenomenology must find some expression or source in the structure of these mathematical objects. This view is advocated here, with arguments and examples to link coherent structures to some of the commonly known characteristics of strange attractors. Fundamental to this link is a geometric interpretation of conditional sampling techniques used to "educe" coherent structures, which offers an explanation for their appearance in measurements as well as their size.

Development of the link between attractors and structures first requires a brief discussion of both structures and conditional sampling techniques, as well as dynamical systems theory. Following this, a generic sampling technique is applied to the Lorenz equations to demonstrate the eduction of "coherent structures" from this model system. Attention then focusses on describing the Navier-Stokes equations as a dynamical system, after which the geometrical meaning of the VITA technique(Blackwelder & Kaplan, 1976) and Quadrant analysis(Lu & Willmarth, 1973) within this system is explained. Finally, some comments are made regarding the arbitrariness of the sampling process and the implications for questions of significance.

COHERENT STRUCTURES AND COHERENT SAMPLING

Historically, the view that turbulent flow contains structure has arisen from flow visualization studies. Two better known examples of this are the bubble pictures of Kim, Kline & Reynolds(1969) in the sublayer of a turbulent boundary layer, and the shadowgraph pictures of Brown & Roshko(1974) in the mixing layer. In both cases a recognizable sequence of events or physical structures, occurring irregularly, could be identified in the pictures. The belief that structures(or sequences) such as these were important to the flow dynamics led to the desire to extract their signature from the stochastic background for independent study. A problem in pattern recognition resulted, although the formalism and language of that field has rarely been applied(Blackwelder, 1978) to the problem of defining a conditional sampling scheme. In each case investigators first construct a "feature" space from those characteristics they believe are unique to the event or structure. In this they are guided by their sense of what important physical processes are associated with a typical event, and how best to identify such processes when they occur. Thus, choice of features includes an element of arbitrariness. In addition this choice can be affected by the kind, or amount, of data not measured. (Readers are reminded of the story of the blind men examining an elephant. Each touches something the other doesnot; each conjectures the essential nature of the elephant to be that which they touched.) The result of this attempted characterization is a detection criterion that is a function of the features. When applied to available transducer signals, it announces occurrences of an event or structure. Once an event's temporal origin has been determined by this scheme, it is aligned with transducer time histories from other events so that they can be ensemble averaged and the coherent signature extracted. Thus development and application of a conditional sampling scheme follows the sequence: choice of features that are functions of available transducer signals; development of a detection criterion based on the features; application of the criterion to determine event origins; ensemble averaging of transducer signals aligned on event origins.

In the sampling schemes used to date the transducer signals have often been hotwire signals for the velocities U_{ij}(i denotes velocity component, j indexes the physical position of the measurement in an array). From these signals M features, f_n, have been constructed. Thus

$$f_n = f_n(U_{ij}) \tag{1}$$

Typical features have been time and space derivatives of the U_{ij}, as well as powers and short term averages of these quantities. Choosing M features establishes a M-dimensional "feature" space.

The state of the flowfield at the measurement array is characterized in time by a feature vector

$$\vec{\mathbf{f}}(t) = \{f_1(U_{ij}), f_2(U_{ij}), \cdots f_M(U_{ij})\} \tag{2}$$

which sweeps out some trajectory in the feature space. and whose components are the value of the features at each instant. The detection criterion. call it G. is a function of the feature variables. In simple cases it can be written as

$$G(f_i) = 0. \tag{3}$$

Often this represents some surface in the feature space. When the feature trajectory $\vec{\mathbf{f}}(t)$ crosses the surface $G(f_i) = 0$.. an event or structure is signalled. The instant of crossing, or some time referenced to the crossing , becomes the event origin. It is used to align transducer signals or feature traces from different events for ensemble averaging. The result: a time trace "typical" of all qualitatively similar, but randomly occurring. events. Since averaging extracts a non-zero trace from a stochastic background. the average is considered to represent an underlying "coherent" structure, shorn of the incoherent fluctuations which obscured it.

DYNAMICAL SYSTEMS, STRANGE ATTRACTORS AND CONDITIONAL SAMPLING

Consider a system of *ode's*(not necessarily finite)

$$\frac{d\vec{\mathbf{X}}}{dt} = h(\mathbf{X}) \tag{4}$$

$$\vec{\mathbf{X}} = (X_1(t), X_2(t). X_3(t), \cdots) \tag{5}$$

With the initial condition

$$\vec{\mathbf{X}}_0 = (X_1(0), X_2(0), X_3(0), \cdots)$$

the solution to the system (4) can be written

$$\vec{\mathbf{X}} = \Phi_{X_o}(\vec{\mathbf{X}}) = \vec{\Phi}_{X_0}(t) \ , \tag{6}$$

or

$$X_i = \Phi_i(t)$$

$\vec{\mathbf{X}}$ is the phase space or "state" variable. Each point on the solution trajectory $\vec{\mathbf{X}} = \vec{\Phi}_{X_0}(t)$ completely characterizes the configuration of the system at an instant.

If the system of *ode's* (4) has only two members, the time asymptotic behavior of $\vec{\mathbf{X}}$ has only three possibilities: steady state, periodic motion, divergence. If the

system is dimension three or greater, and is dissipative (the trace of the Jacobian matrix $[\partial h_i/\partial X_j] < 0$), then the asymptotic solution may be confined to a "strange attractor" in the phase space. Solutions confined to strange attractors are almost everywhere locally unstable, but are globally stable to perturbations which do not cross the bounds of their basins of attraction. Thus system states which are initially nearby diverge exponentially from each other for short times. Trajectories on strange attractors never repeat themselves exactly, but ultimately will pass arbitrarily close to any previous portion of the trajectory.

Consider the character of a bundle of trajectory segments which all pass through some "window" in the space of the attractor. If the window is small enough, the system states occurring on each trajectory segment at the instant of passage through the window will all be similar. The sequence of states along each segment remains correlated with those along other segments for some time after (and before) passage through the window. However, exponential divergence of nearby trajectories guarantees that this correlation time is finite. An ensemble average over trajectories passing through the window, and aligned on the window passage time, will yield a non-zero trace over finite time for any phase space component(or function of them) which has a zero mean value.

The above concepts are illustrated in Figures 1-3. The strange attractor which represents the asymptotic solution to the Lorenz system for a particular set of parameter values is pictured in Figure 1a. The X-Z plane intersects the attractor transversely, and a large rectangular window has been outlined in this plane. Each time the solution trajectory passes through the window, the next 500 points in the time series of the Y component of the solution are traced in Figure 1b. In Figure 1c the ensemble average of the 152 traces so obtained is displayed. Because the window is large the selected traces are not substantially correlated with each other. Despite the fact their Y coordinates are identically zero at window passage, the range of X and Z values at intersection means that the system states (X,Y,Z) are "far" apart. In Figure 2 the window area has been decreased by a factor of five, and the correlation between selected traces increases substantially. The ensemble average now clearly shows a non-zero value for finite time after passage. A further decrease in window size, now barely discernible in Figure 3, again reduces the number of traces selected from a given record length, but sharpens their correlation. The non-zero portion of the average increases both in duration and peak magnitude as a result.

It is easy to see that the "window" constitutes a conditional sampling criterion in the phase space of the Lorenz attractor. Here the "features" are the primitive variables (X,Y,Z) themselves, and the detection criterion, though not in the form of equation (3), is a simple function of the features, namely

$$Y = 0.$$

$$a \leq X \leq b \qquad (7)$$

$$c \leq Z \leq d$$

The event criterion (7) simply chooses the bundle of trajectories on the attractor which are ensemble averaged. If the detection criterion is too broad, selected trajectory segments are uncorrelated to begin with, and averaging fails to extract a structure. Tightening the selection criteria(decreasing the window size) increases the likelihood that trajectory segments are initially correlated, but exponential divergence of trajectories on the attractor guarantees that their mutual correlation time is finite. At times beyond the correlation limit, the ensemble average of the trajectories will be zero. If the size of a structure is defined as the length of non-zero trace which results from averaging, then the tighter the selection criterion, the greater the size of the educed event. Given the minimum distance, Δ, between trajectories at the event window, information theory(Shaw,1981) suggests that an upper bound on the event size or duration is given by a constant times the logarithm of $1/\Delta$. This separation between trajectories must be calculated in the full phase space of the dynamical system, not in some reduced dimension feature space.

THE NAVIER-STOKES EQUATIONS AS A DYNAMICAL SYSTEM AND APPLICATIONS OF CONDITIONAL SAMPLING TO ITS SOLUTIONS

Constructing the link between coherent structures measured by experimentalists and their hypothesized origin in the structural details of an attractor requires that the Navier-Stokes equations can be considered a dynamical system in the form (4), and that its solutions are confined to a strange attractor. The first is shown below. For the second, there are rigorous results to prove that solutions to the two-dimensional Navier-Stokes equations are confined to a finite dimensional attractor(Constantin & Foias ,1985). Similar rigor has not yet been obtained in the three-dimensional case. However, the author has performed calculations on low Reynolds number, turbulent channel flow which indicate, at least in this important case, that solutions to the three-dimensional Navier-Stokes equations are confined to a finite (but large) dimension strange attractor(Keefe et al., 1987). The point may not be proven, but the circumstantial evidence is strong.

Formally, the Navier-Stokes equations are an infinite dimensional system because they require functional, rather than discrete, initial data. However, through the practice of disretization, both experiments and numerical simulation project the system onto a finite one. An experimenter examines a finite volume of flow, and makes measurements of flow quantities at a finite number of points. A numerical simulation operates in a computatioinal domain which may be infinite, but flow quantities are calculated at a finite number of points(the grid) within it.

Imagine a phase space vector $\vec{\mathbf{S}}$ whose components are the flow velocities u, v, w at N different points in space

$$\vec{\mathbf{S}} = (u_1, v_1, w_1, u_2, v_2, w_2, \cdots u_N, v_N, w_N) \tag{8}$$

Spatial discretization schemes(finite difference, collocation) applied to the Navier-Stokes equations will yield a finite dimensional dynamical system

$$\frac{d\vec{\mathbf{S}}}{dt} = g(\vec{\mathbf{S}}) \tag{9}$$

The right hand side of each member of equation (9) will have terms linear in the velocities due to viscosity, and two kinds of nonlinear terms. The first are due to the convective terms, and couple nearby velocities together through their space derivatives. The second kind will be due to the pressure gradient, and globally couple all components together in incompressible flow. As the number of points at which velocities are known increases towards infinity, system (9) becomes equivalent to the Navier-Stokes in the sense that each requires the same initial data, and solution of either gives the entire flow field.

Because of discretization neither experiments nor calculations have access to the full dynamical system represented by (9) as $N \rightarrow \infty$. Making a single point measurement of one velocity component records the solution to but one equation from the infinite dimensional system. It is impossible to characterize the entire quantitative state of a multidimensional dynamical system by looking at only one of its components. However, in theory(Packard et al.,1980, Takens, 1981), it is possible to recover the full qualitative behavior of a system from one of its components by use of embedding techniques. Conceptually, then, it is possible to characterize an entire flow field from one hotwire measurement, provided that one time history can be processed enough to yield sufficient numbers of independent coordinates. If they are sufficient, the qualitative dynamics of the flow on its attractor are reproduced on a different attractor in this new phase space.

With more hotwire measurements fewer additional independent coordinates need be derived for a complete description, but enough that the qualitative dynamics are reproduced. Given the choice between describing a system by ten coordinates derived from a single measurement of a primitive variable, or ten coordinates each of which is a different primitive measurement, the latter is the better choice. Both should give the same qualitative description of the dynamics, but the second also provides a quantitative description.

It is important to realize that discretization is a projection process, and that in this process quantitative information about the system under study is obscured or lost. Construction of a "feature" space for event recognition is such a discretization. It projects the full solution attractor onto a reduced dimension phase space and may make inaccessible the phase coordinates needed to discriminate between

apparently similar states. In applications of conditional sampling techniques to discrete numbers of hot wire signals this loss produces the phase jitter and temporal misalignment problems which reduce coherence between events, and which may require extensive iterative processing of the signals for a structure to be educed (Hussain, 1983).

In light of the previous paragraphs, eduction of coherent structures by conditional sampling can be viewed as the following set of operations on the full solution attractor of the Navier-Stokes equations. First, discretization of the flow field collapses the full attractor onto a reduced dimension subspace. Second, a "feature" space is constructed out of components from this subspace, or functions of them. The number of features selected determines the dimension of the new space, which may actually be higher than that resulting from the discretization. This new space contains a finite size object to which the feature trajectory is confined, but this object is not an attractor in the rigorous sense. Third comes construction or specification of an event criterion in the feature space. The criterion is a subset of the feature space(curve, surface, surface patch, etc.), but may be infinite in extent. Fourth, the intersection points between the feature trajectory and the event criterion are determined. Finally, an ensemble average of primitive, or feature, traces aligned on these intersection points is obtained. Using velocity signals derived from numerical simulations of low Reynolds number channel flow (Kim, Moin & Moser, 1987) these processes are illustrated for both the VITA technique and Quadrant analysis, two conditional sampling schemes which have played important roles in studies of near wall structure.

In Blackwelder and Kaplan's 1976 application of the VITA technique discretization of the flow field projected the full attractor onto a one dimensional subspace, namely a single hotwire measurement at $y^+ = 15$. A two dimensional feature space was constructed from this signal using the moving average operation on the raw signal and its square. Thus the feature coordinates were

$$U_{lm}(t) = \frac{1}{T} \int_{t-\frac{T}{2}}^{t+\frac{T}{2}} U(\tau) d\tau \tag{10}$$

$$U_{lm}^2(t) = \frac{1}{T} \int_{t-\frac{T}{2}}^{t+\frac{T}{2}} U^2(\tau) d\tau$$

An additional constant was derived, the meansquare value

$$U_{ms} = \lim_{T \to \infty} U_{lm}^2$$

The sampling criterion was the parabola

$$U_{lm}^2 = (U_{lm})^2 + k_1 U_{ms} \tag{11}$$

where k_1, the threshold constant, had a value 1.2. Passage of the feature trajectory from outside the parabola to inside signalled an event. The temporal origin of the event was assigned to the midpoint of the trajectory's residence within the parabola. Figures 4-6 illustrate the geometry of this scheme.

Figure 4 shows the effect of using too short an averaging time to create the feature coordinates. As the averaging time T in equation (10) approaches zero, the feature trajectory will become a plot of $U^2(t)$ against $U(t)$. This will be a parabola opening upwards with vertex at the origin. The sampling criterion (11) is always a similar shaped parabola whose vertex has been displaced upwards from the origin an amount dependent upon k_1. Since the two parabolas are the same shape, the feature trajectory can never intersect the event criterion in this case. Such a situation can be seen in Figure 4a.

Figure 5 shows the VITA technique using values of k_1 and T similar to those in Blackwelder and Kaplan. In Figure 5a the feature trajectory and event criterion are plotted. Increasing the averaging time now causes the feature trajectory to occasionally cross the parabola. Each time it does the 300 time points of $U(t)$ centered around the event origin are plotted in 5b, and the origin is marked on the time line in 5d by a vertical tick. Figure 5c shows the ensemble average of the aligned events. It should be noted that the Reynolds number of the simulation data is much lower than that of the boundary layer employed in the original measurements. The measured bursting frequency, and the amplitude of the ensemble average, are lower than found by Blackwelder, but the shape and duration of the event are similar. Here the vertical tick marks on the average plot represent the rms value of $U(t)$. More important than these comparisons however, is the relation between the shape of the feature trajectory and the sampling criterion. With very high probability, the feature trajectory retains a parabolic character even with longer averaging times. The event criterion is essentially parallel to this "fuzzy" parabola in feature space, so the chances of intersection are low. Those intersections that do occur cover a wide range of the feature coordinates. This suggests that the events detected are not "close" to each other in the full phase space, and may decorrelate rapidly. With this feature trajectory the detector isn't sharp and doesnot necessarily pick out high probability events. However, multiplying the burst duration times the number of events suggests that some part of the process is going on 25% of the time.

In later work Blackwelder and Haritonidis(1983) sharpened the detection criterion by adding a third feature coordinate: $\partial U/\partial t$. They chose to select only those events for which $\partial U/\partial t > 0$. In this case the feature trajectory is a space curve, and the event criterion is that half of a parabolic cylinder which extends into positive $\partial U/\partial t$ space. Figure 6 shows this scheme projected back onto two dimensions. Fewer events are detected from the same time history, but their correlation is sharper, with the result that the ensemble average has a larger peak amplitude.

In an early study of the bursting process Lu & Willmarth invented the technique of Quadrant analysis. Here discretization projects the full attractor down to a 2-space consisting of U and V measurements at $y^+ = 15$. The primitive velocities are also the feature variables in this case. Two constants, the rms values of U and V, are formed. Then the event criterion is a rectangular hyperbola in hodograph(U,V) space

$$UV = -k_2 U_{rms} V_{rms} \tag{12}$$

A further distinction on events detected by this scheme was to separate the quadrant 2(bursts) events from those in quadrant 4(sweeps). Figure 7 displays this scheme applied to the same velocity fields used for the VITA technique. A threshold constant $k_2 = 4.$(within the range used by Lu and Willmarth) is used, and only quadrant 2 events have been selected. Again the 300 time points of U(t) centered on the event are plotted in 7b. Clearly the temporal behavior of the event selected here is different from that chosen by VITA. However, comparison of the time lines shows that the two schemes do choose events at roughly the same time, occasionally almost exactly. In contrast to VITA, Quadrant analysis seems to be a sharper detector, since the feature trajectory at $y^+ = 15$ is more transverse to the detector that parallel. This produces a tighter clustering of feature states at the event window. While such continues to be true for velocities measured at greater distances from the wall, it is not true for those measured at lesser distances, because the smallness of V makes the feature trajectory almost parallel to the U axis. In addition, clustering in feature space is no surety for similar behavior in the full phase space. Thus sharpness of this kind may be an entirely spurious indicator of goodness in a detector.

CONCLUSIONS

Discretization connects the feature space of a conditional sampling technique to subspaces of the full solution attractor of the Navier-Stokes equations. A geometric interpretation of the sampling criterion, coupled to the exponential divergence property of trajectories on strange attractors, provides an explanation for the measurement of "structure" in turbulence. The sampling criterion selects a group of nearby trajectories on the attractor for ensemble averaging. Their nearness implies a certain mutual correlation initially, but exponential spreading guarantees the correlation time will be finite. This correlation time can be increased by sharpening the criterion. An ensemble average thus produces a finite duration event or structure. The choice of the sampling criterion is essentially arbitrary. An enormous amount of flow information can be lost by the discretization process, so each investigator attempts to recover some of it by perceptive design of the sampling criterion. Carried to its logical extreme, it is clear that any sufficiently restrictive sampling criterion will extract a structure from a dynamical process confined to a strange attractor. If structures are defined as those objects which can be extracted by conditional sampling criteria, then they are everywhere one looks in

turbulence. Some idea of this arbitrariness is obtained by modifying the VITA technique slightly to to see what it will detect.

Write the sampling criterion

$$U_{lm}^2 = A(U_{lm})^2 + k_1 U_{ms} \tag{13}$$

The additional constant A controls the spreading rate of the parabola. Figure 8 shows the result of sampling when the threshold k_1 has been raised to 3., but the parabola has been flattened by letting A=.1. In addition, the moving average has been shortened and only those events where the moving average is negative have been selected. Equation (13) no longer has a straightforward physical interpretation, but it is sharper as a detector in feature space, and selects more events than unmodified VITA. By coincidence the "structure" it educes is very similar to that obtained by Quadrant analysis.

Arbitrariness in the selection process begs the question of significance. There is structure in turbulence. However, it is up to each investigator to supply the physical arguments which raise their ensemble average to the status of a structure which contributes significantly to the dynamics of the flow.

ACKNOWLEDGEMENTS

The author is indebted to S. K. Lele and R. D. Moser for both stylistic and conceptual clarifications of the manuscript. This research supported, in part, by the Air Force Office of Scientific Research, under contract AFOSR-88-0056.

REFERENCES

Blackwelder, R. F. & Kaplan, R. E., 1976, On the Wall Structure of the Turbulent Boundary Layer. *J. Fluid Mech.*. **76**, p.89

Blackwelder, R. F., 1979, Eddy Detection Within Turbulent Flows. *Proceedings of the Dynamic Flow Conference, Skovlunde, Denmark*

Blackwelder, R. F. & Harotinidis, J. H., 1983, Scaling of the Bursting Frequency in Turbulent Boundary Layers. *J. Fluid Mech.*. **132**, p.87

Brown, G. L. & Roshko, A., 1974, On Density Effects and Large Structures in Turbulent Mixing Layers. *J. Fluid Mech.*. **64**, p.775

Constantin, P. & Foias, C., 1985, Global Lyapunov Exponents, Kaplan-Yorke Formulas and the Dimension of Attractors for the Navier-Stokes Equations. *Comm. Pure Appl. Math.*. **38**, p.1

Hussain, A.K.M.F., 1983. Coherent Structures-Reality and Myth. *Phys. Fluids.* **26**, p.2816

Keefe, L., Moin, P. & Kim, J., 1987. The Dimension of an Attractor in Turbulent Poiseuille Flow. *Bull. A.P.S.* **32**, p.2026

Kim, H. T., Kline, S. J. & Reynolds, W. C., 1971. The Production of Turbulence Near a Smooth Wall in a Turbulent Boundary Layer. *J. Fluid Mech.*, **50**, p.133

Kim, J., Moin, P. & Moser, R., 1987. Turbulence Statistics in Fully Developed Channel Flow at Low Reynolds Number. *J. Fluid Mech.*, **177**, p.133

Lu, S. S. & Willmarth, W. W., 1973. Measurements of the Structure of the Reynolds Stress in a Turbulent Boundary Layer. *J. Fluid Mech.*, **60**, p.481

Packard, N. H., Crutchfield, J. P., Farmer, J. D. & Shaw, R. S., 1980, Geometry From a Time Series. *Phys. Rev. Lett.*, **45**, p.712

Shaw, R. S., 1981, Strange Attractors, Chaotic Behavior, and Information Flow. *Z. Naturforsch.*, **36a**, p.80

Takens, F., 1981, Detecting Strange Attractors in Turbulence. *Lecture Notes in Mathematics, Springer-Verlag.* **898**, p.366

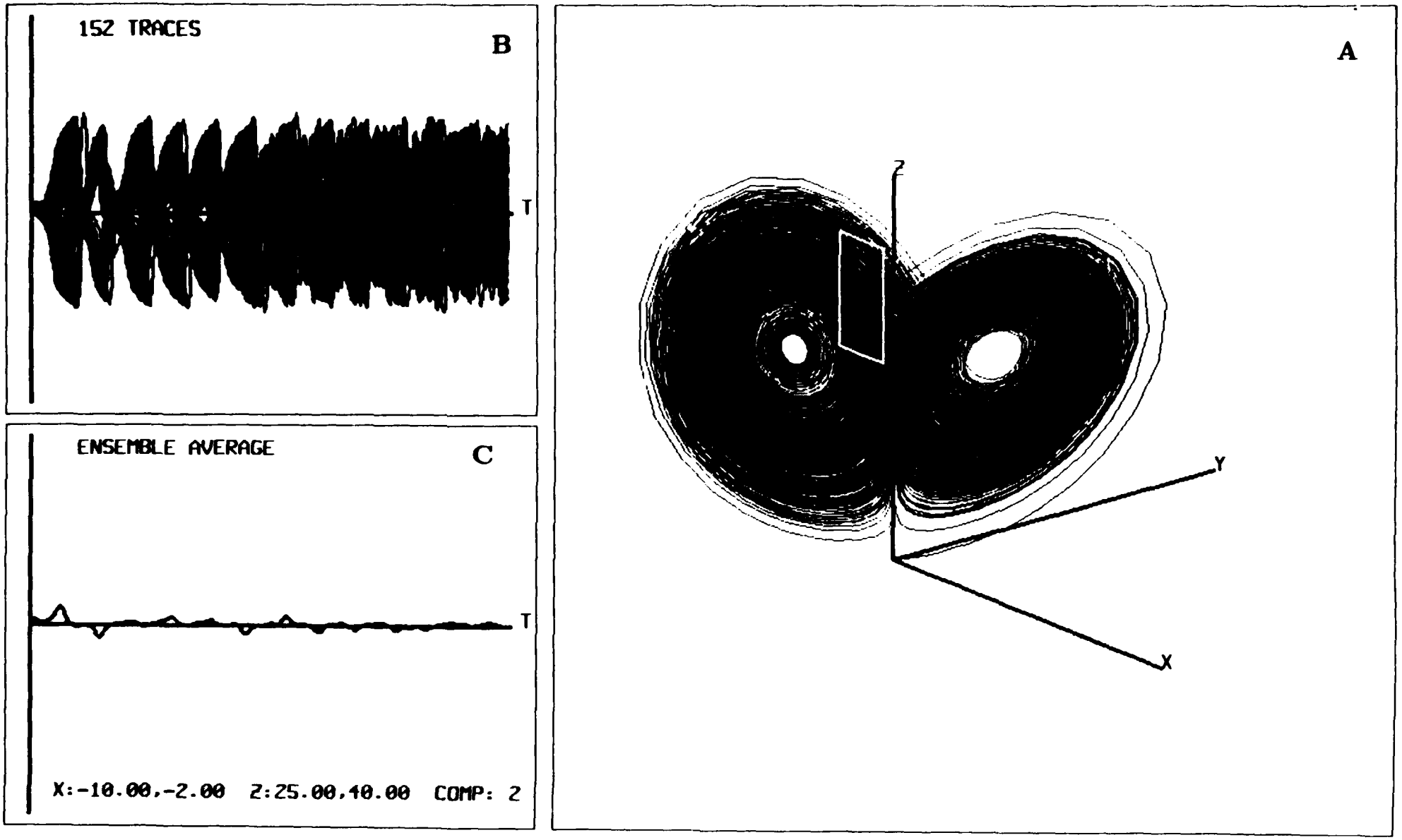

Figure 1: a) Lorenz attractor with window $-10 < X < -2$, $25 < Z < 40$. b) Aligned Y traces. c) Ensemble average of Y traces.

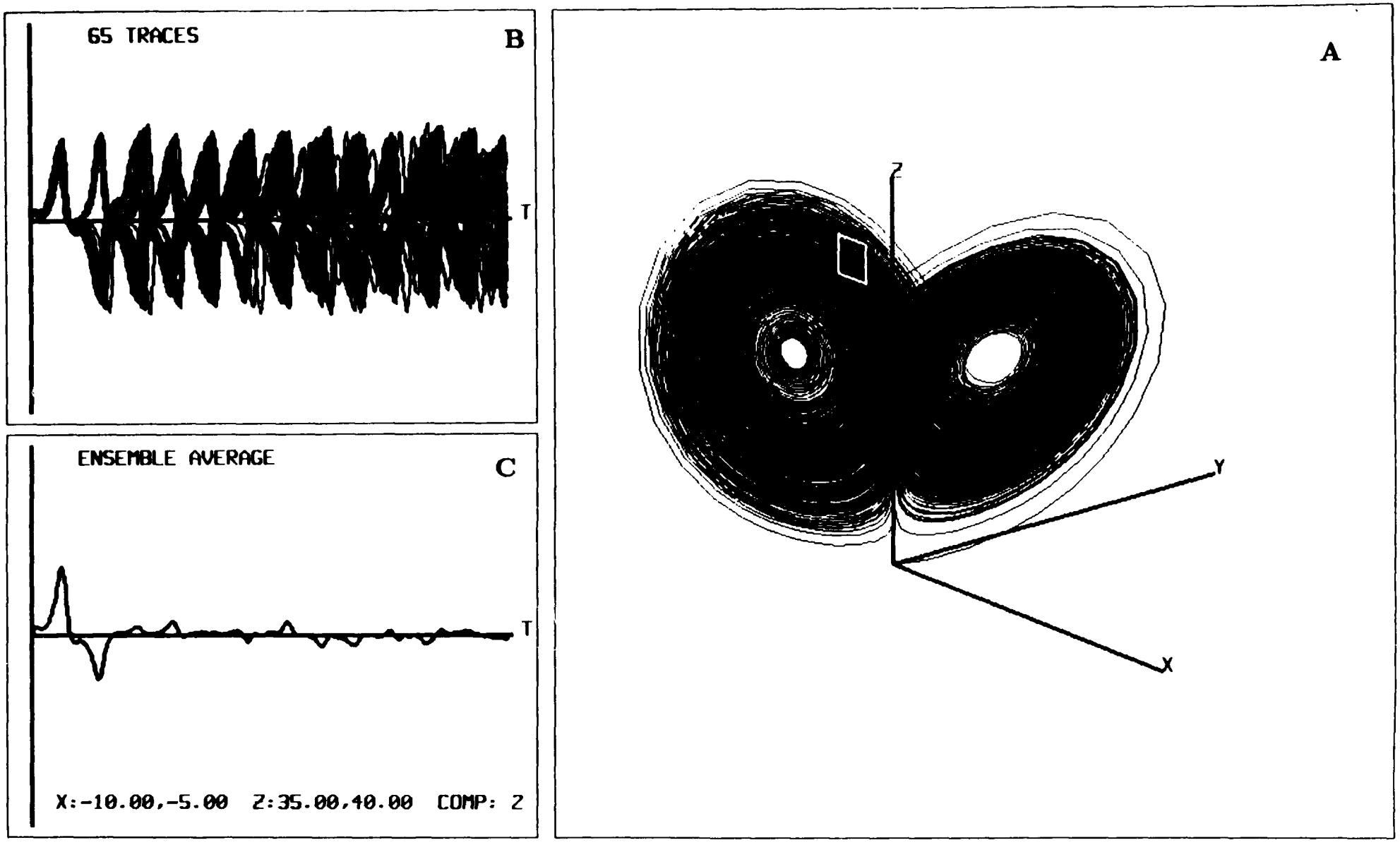

Figure 2: a) Lorenz attractor with window $-10 \leq X \leq -5$, $35 \leq Z \leq 40$. b) Aligned Y traces. c) Ensemble average of Y traces.

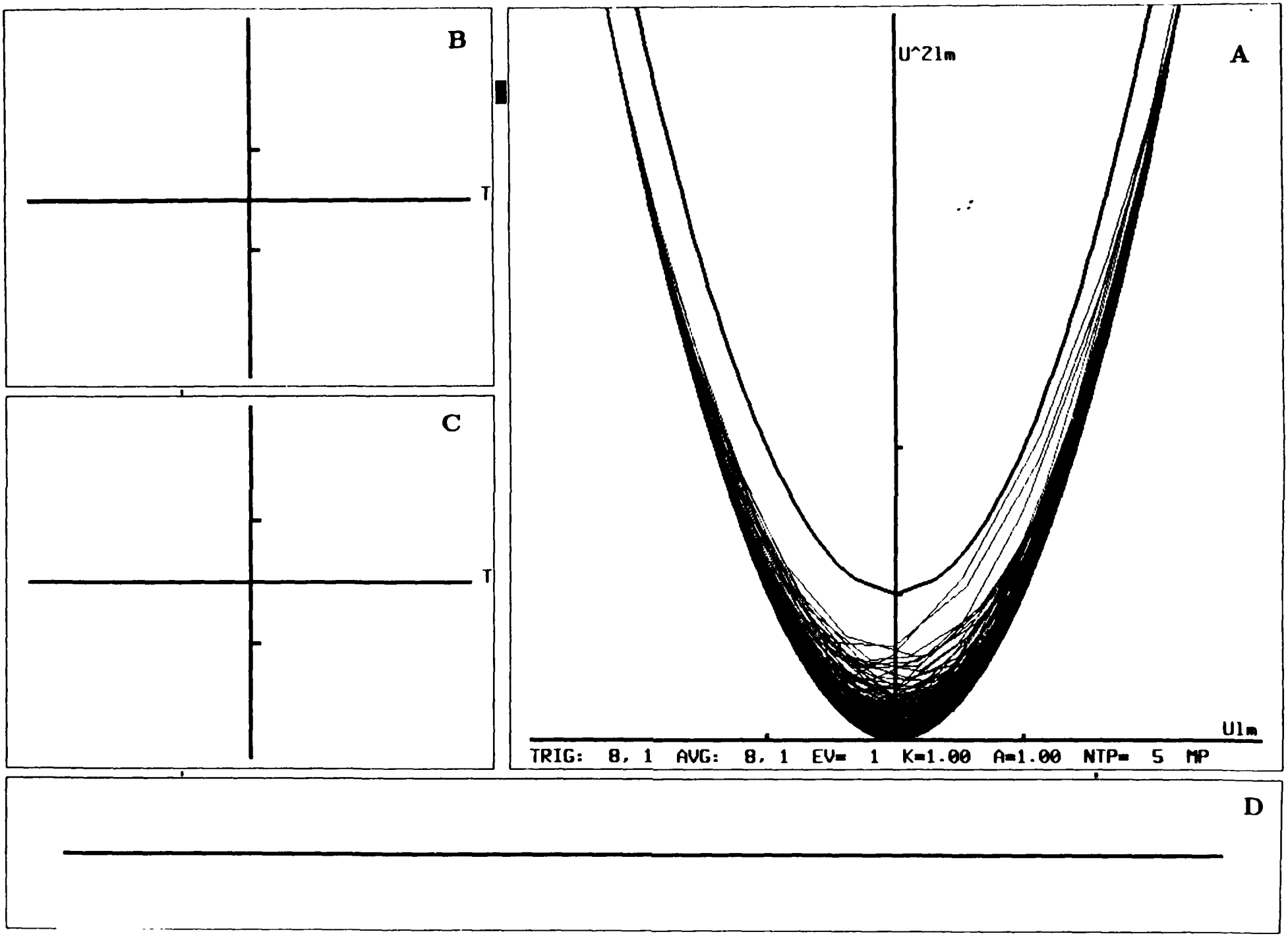

Figure 4: VITA technique, $Tu_\tau^2/\nu = 3.45$, $k_1 = 1.2$ a) Feature trajectory and parabolic event criterion. b) Aligned U' traces. c) Ensemble average of U' traces. d) Timeline of event origins.

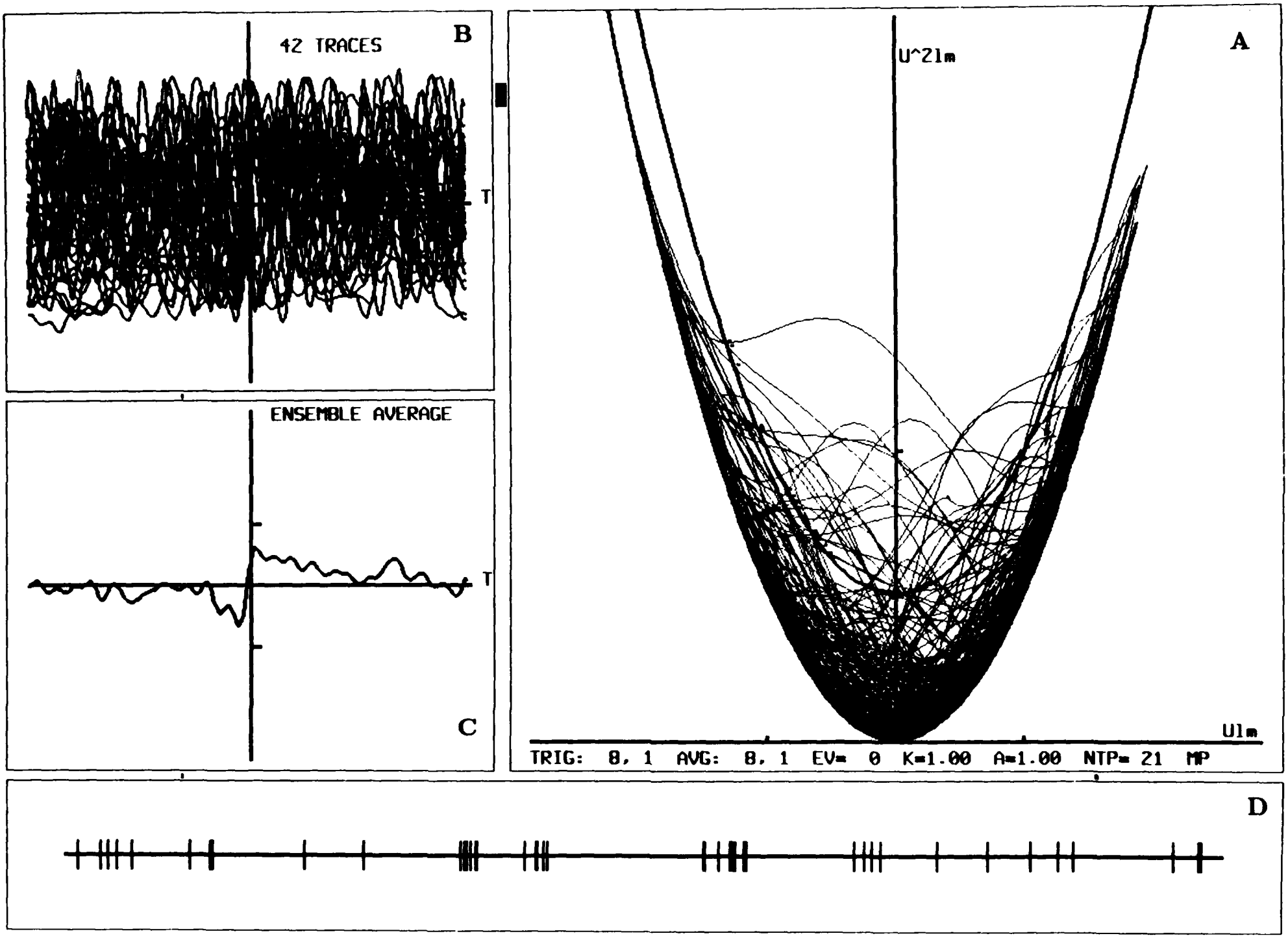

Figure 5: VITA technique, $Tu_\tau^2/\nu = 14.5$, $k_1 = 1.2$ a) Feature trajectory and parabolic event criterion. b) Aligned U'

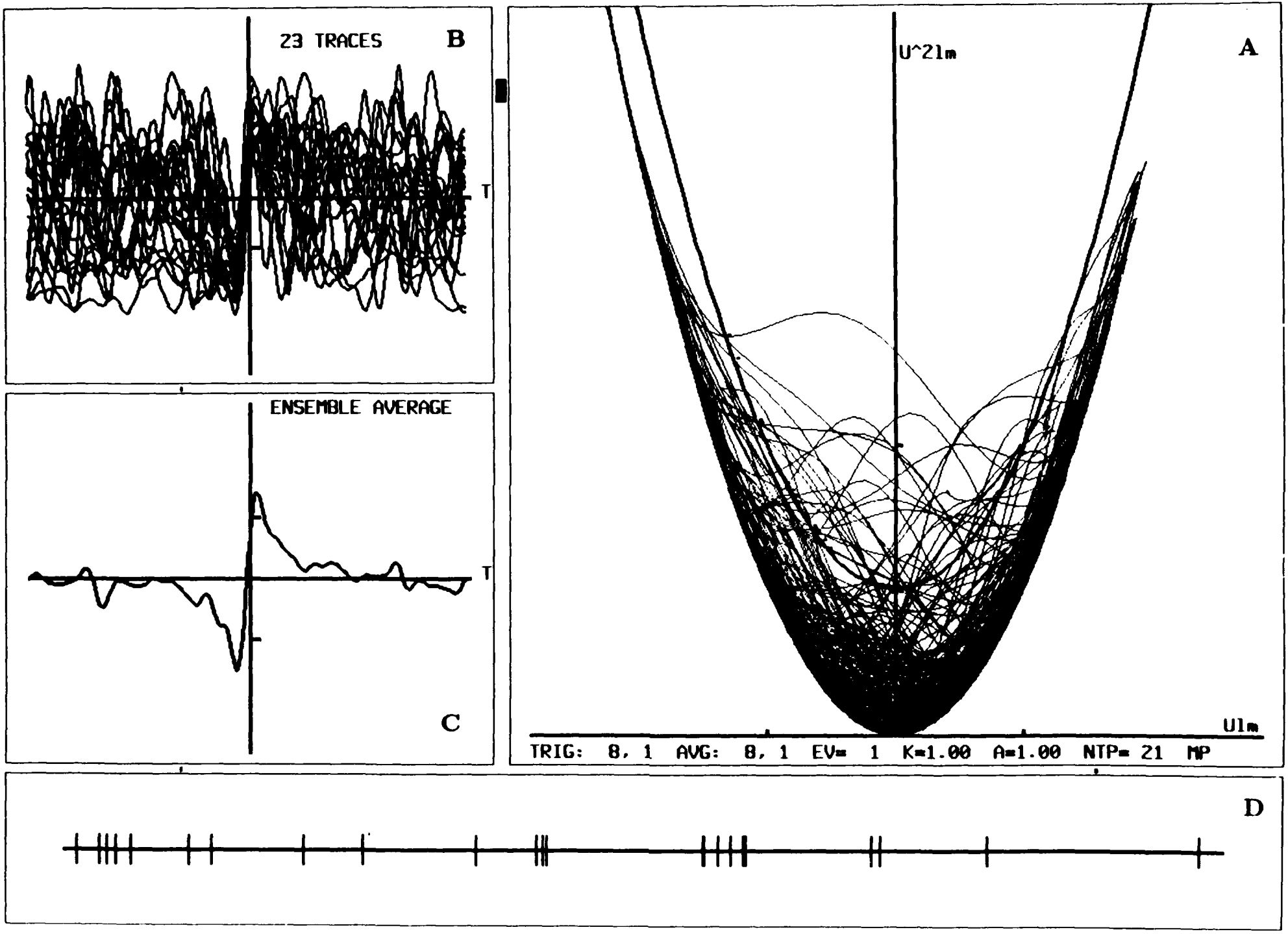

Figure 6: VITA technique, $Tu_\tau^2/\nu = 14.5, k_1 = 1.2$, $\partial U/\partial t > 0$ a) Projection of feature trajectory and parabolic cylinder event criterion. b) Aligned U' traces. c) Ensemble average of U' traces. d) Timeline of event origins.

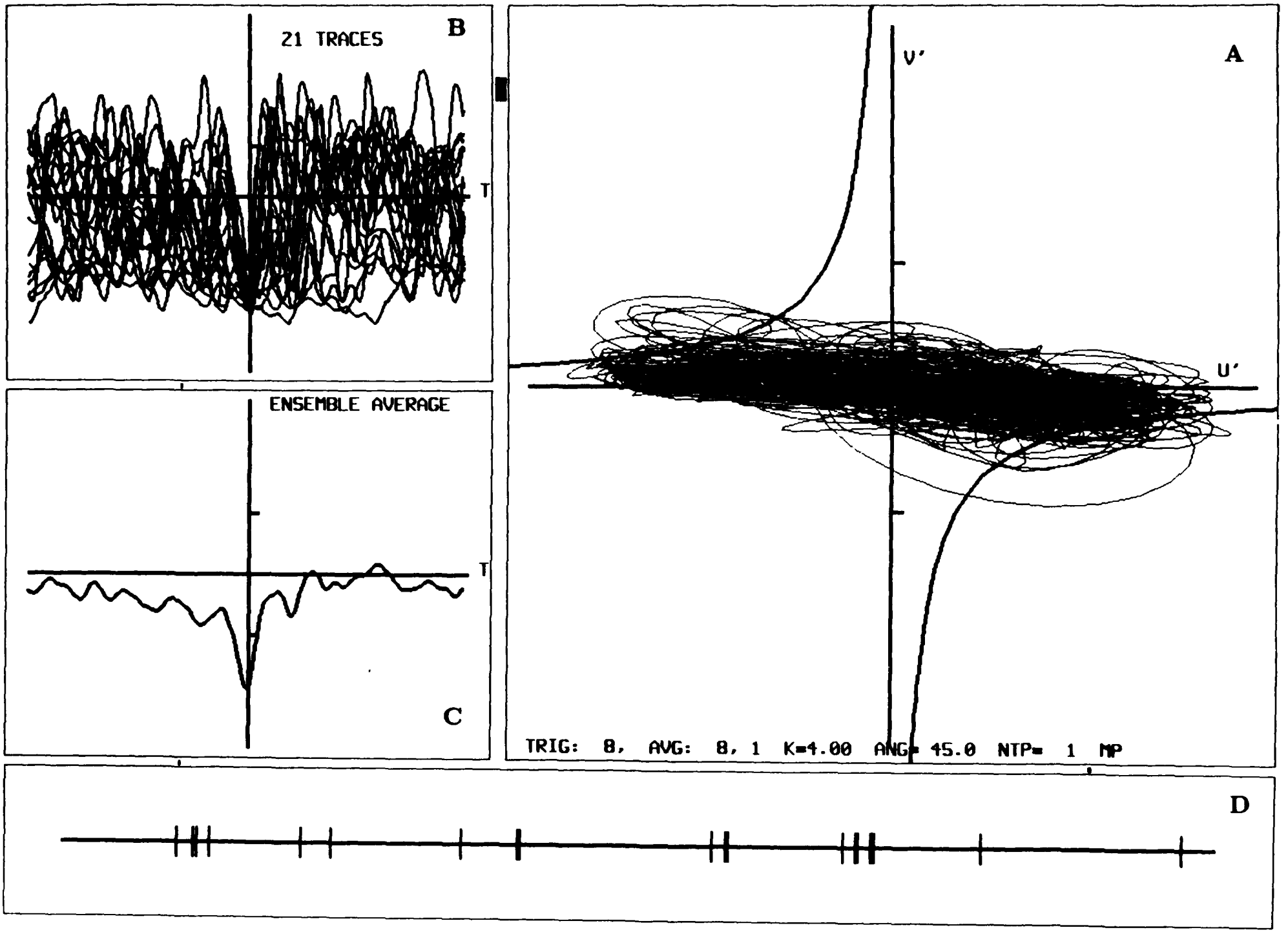

Figure 7: Quadrant analysis, $k_2 = 4$, quadrant 2 events only a) Feature trajectory and hyperbolic event criterion. b) Aligned U' traces. c) Ensemble average of U' traces. d) Timeline of event origins.

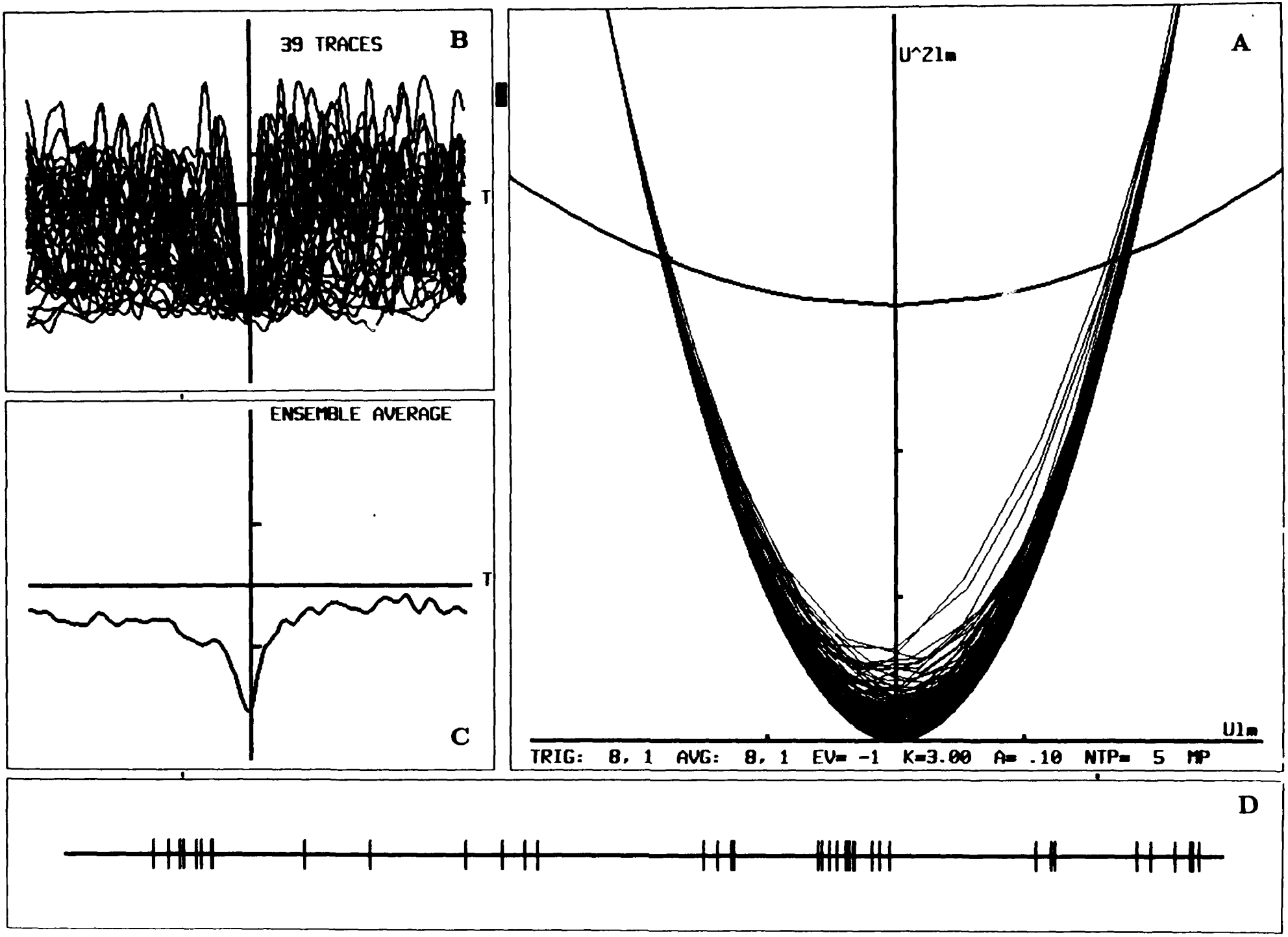

Figure 8: Modified VITA technique, $Tu_\tau^2/\nu = 3.45$, $k_1 = 3.$, $A = .1$ a) Feature trajectory and parabolic event criterion. b) Aligned U' traces. c) Ensemble average of U' traces. d) Timeline of event origins.